Ganymede MHD Model: Magnetospheric Context for Juno's PJ34 Flyby

Stefan Duling[1], Joachim Saur[1], George Clark[2], Frederic Allegrini[3], Thomas Greathouse[3], Randy Gladstone[3,4], William Kurth[5], John E. P. Connerney[6,7], Fran Bagenal[8], Ali H. Sulaiman[9]

[1]Institute of Geophysics and Meteorology, University of Cologne, Cologne, Germany
[2]The Johns Hopkins University Applied Physics Laboratory, Laurel, Maryland, USA
[3]Southwest Research Institute, San Antonio, Texas, USA
[4]University of Texas at San Antonio, San Antonio, Texas, USA
[5]Department of Physics and Astronomy, University of Iowa, Iowa City, Iowa, USA
[6]NASA Goddard Space Flight Center, Greenbelt, Maryland, USA
[7]Space Research Corporation, Annapolis, Maryland, USA
[8]Laboratory for Atmospheric and Space Physics, University of Colorado, Boulder, Colorado, USA
[9]School of Physics and Astronomy, Minnesota Institute for Astrophysics, University of Minnesota, Minneapolis, Minnesota, USA

Key Points:

- Our MHD model illustrates the state of Ganymede's magnetosphere during Juno's flyby and locates its trajectory outside closed field lines.
- The location of the open-closed-field line-boundary is predicted and matches the poleward edges of the aurora as observed by Juno.
- We investigate model uncertainties caused by incomplete knowledge of upstream conditions and other parameters.

Corresponding author: Stefan Duling, `stefan.duling@uni-koeln.de`, `https://orcid.org/0000-0001-7220-9610`

Abstract

On June 7th, 2021 the Juno spacecraft visited Ganymede and provided the first in situ observations since Galileo's last flyby in 2000. The measurements obtained along a one-dimensional trajectory can be brought into global context with the help of three-dimensional magnetospheric models. Here we apply the magnetohydrodynamic model of Duling et al. (2014) to conditions during the Juno flyby. In addition to the global distribution of plasma variables we provide mapping of Juno's position along magnetic field lines, Juno's distance from closed field lines and detailed information about the magnetic field's topology. We find that Juno did not enter the closed field line region and that the boundary between open and closed field lines on the surface matches the poleward edges of the observed auroral ovals. To estimate the sensitivity of the model results, we carry out a parameter study with different upstream plasma conditions and other model parameters.

Plain Language Summary

In June 2021 the Juno spacecraft flew close to Ganymede, the largest moon of Jupiter, and explored its magnetic and plasma environment. Ganymede's own magnetic field forms a magnetosphere, which is embedded in Jupiter's large-scale magnetosphere, and which is unique in the solar system. The vicinity of Ganymede is separated into regions that differ in whether the magnetic field lines connect to Ganymede's surface at both or one end or not at all. These regions are deformed by the plasma flow and determine the state of the plasma and the location of Ganymede's aurora. We perform simulations of the plasma flow and interaction to reveal the three-dimensional structure of Ganymede's magnetosphere during the flyby of Juno. The model provides the three-dimensional state of the plasma and magnetic field, predicted locations of the aurora and the geometrical magnetic context for Juno's trajectory. These results are helpful for the interpretation of the in situ and remote sensing obtained during the flyby. We find that Juno did not cross the region with field lines that connect to Ganymede's surface at both ends. Considering possible values for unknown model parameters, we also estimate the uncertainty of the model results.

1 Introduction

As the largest moon in the solar system, Ganymede not only resides inside Jupiter's huge magnetosphere but also possesses an intrinsic dynamo magnetic field (Kivelson et al., 1996). The co-rotating Jovian plasma overtakes Ganymede in its orbit with sub-alfvénic velocity and drives an interaction that is unique in the solar system. The internal field acts as an obstacle for the incoming plasma flow, generating plasma waves, Alfvén wings and electric currents along the magnetopause (Gurnett et al., 1996; Frank et al., 1997; Williams et al., 1997). The incoming Jovian magnetic field reconnects at the boundary of a donut-shaped equatorial volume of closed field lines that are defined by both ends connecting to Ganymede's surface (Kivelson et al., 1997). The open field lines in the polar regions connect to Jupiter at the other end and define the extent of Ganymede's magnetosphere. Near the open-closed-field line-boundary (OCFB) observations by Hubble Space Telescope (HST) revealed the presence of two auroral ovals within Ganymede's atmosphere (Hall et al., 1998; Feldman et al., 2000).

On June 7th, 2021 Juno approached Ganymede from the downstream side and crossed the magnetospheric tail for the first time. Juno encountered Ganymede with a minimum distance of 1046km (∼0.4 radii) on a trajectory heading northwards and towards Jupiter, leaving the interaction system at its flank (Hansen et al., 2022).

For analyzing and interpreting the measurements obtained by Juno (Allegrini et al., 2022; Clark et al., 2022; Kurth et al., 2022) it is important to study which part of its trajectory is geometrically related to the various regions of Ganymede's magnetosphere.
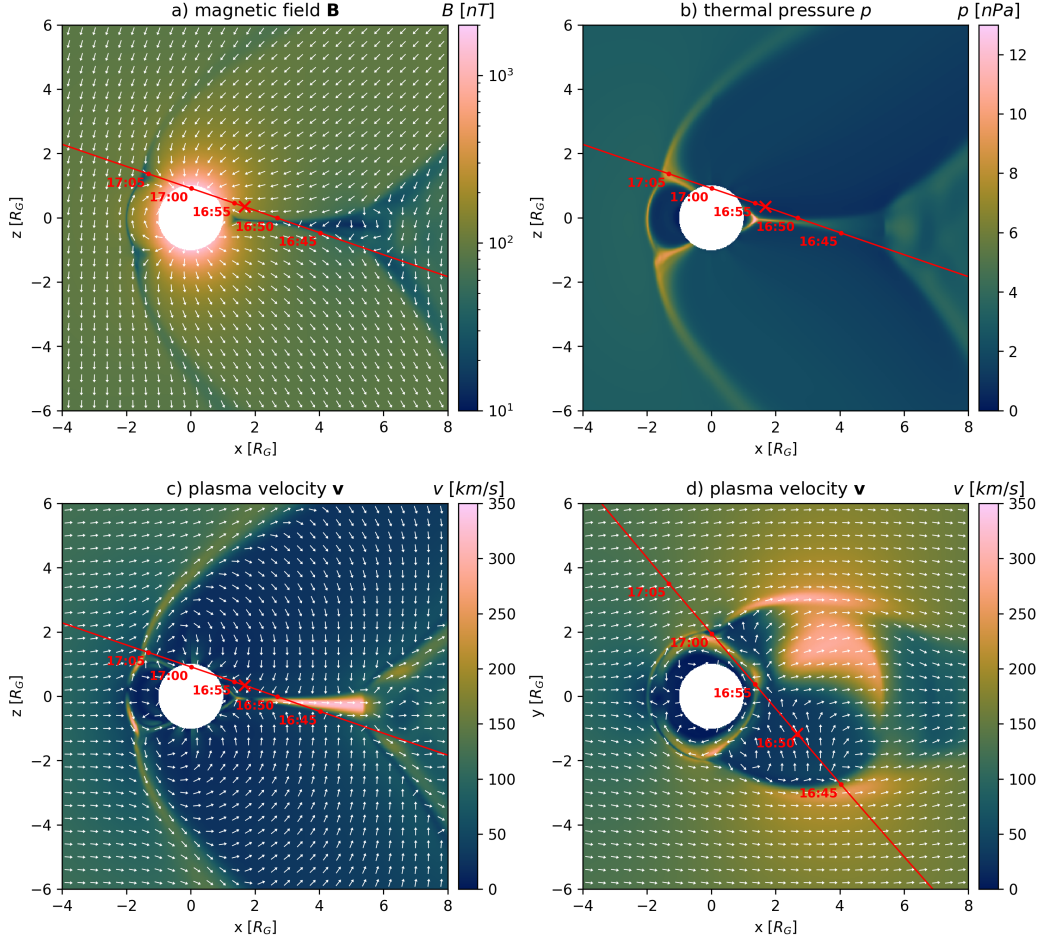
Figure 1. Model variables for Juno's flyby, plasma flow from left to right. $y{=}0$ plane: a) Magnetic field **B**, b) thermal pressure p, c) velocity v. Equatorial plane, $z{=}0$: d) velocity **v**. The red crosses indicate Juno's crossing through these planes and the red lines the projected trajectory. The white arrows show the projected direction of **B** and **v** respectively. Figures S3-S4 show planes with minimized trajectory projection.

Juno's measurements could not uniquely conclude whether Juno crossed the closed field line region. For example, JEDI found double loss cones for >30keV electrons (Clark et al., 2022) while JADE found only single loss cones (Allegrini et al., 2022). To find the location where detected particles can interact with Ganymede's atmosphere or surface, i.e. Juno's magnetic footprint, the necessary field line tracing requires a model for the magnetic field. Furthermore, Juno's UVS instrument provided auroral images at unprecedented resolution (Greathouse et al., 2022). Electron acceleration processes driving Ganymede's aurora are not fully understood, however, from analysis of poorly resolved HST observations it was argued that the aurora occurs near the OCFB (McGrath et al., 2013). To substantiate this previous finding a comparison of the Juno UVS observations with the modeled magnetic topology is of considerable interest. The aim of this work is thus to provide field and mapping properties during the flyby and illustrate the three-dimensional context of Juno's measurements (Section 3). We further carry out a model sensitivity study on uncertain upstream conditions and other model parameters to estimate their impact and the uncertainty of our results (Section 4).

2 Model

We describe Ganymede's space environment by adopting a magnetohydrodynamic (MHD) model based on Duling et al. (2014), which describes a steady state solution for a fixed position in Jupiter's magnetosphere. In our single-fluid approach the plasma interaction is described by the plasma mass density ρ, plasma bulk velocity $\mathbf{v}$, total thermal pressure p and the magnetic field $\mathbf{B}$. For these variables appropriate boundary conditions are applied at Ganymede's surface and at a distance of 70 Ganymede radii ($R_G = 2631$ km). Our model includes simplified elastic collisions with an O_2 atmosphere, ionization processes and recombination. Ganymede's intrinsic magnetic field is described by dipole Gauss coefficients $g_1^0 = -716.8$ nT, $g_1^1 = 49.3$ nT, $h_1^1 = 22.2$ nT (Kivelson et al., 2002). During Juno's visit Ganymede was near the center of the current sheet ($302°$W System-III, $-2°$ magnetic latitude) where the induction response of an expected ocean (Saur et al., 2015) is close to minimum. In our model the induced field has a maximum surface strength of 15.6 nT. The upstream plasma conditions are adjusted to the flyby situation as listed in Table 1. They characterize the interaction to be sub-Alfvénic with an Alfvén Mach number of $M_A = 0.8$ and a plasma beta of 1.1.

While we utilized the ZEUS-MP code (Hayes et al., 2006) in Duling et al. (2014) we now present results obtained with the PLUTO code (Mignone et al., 2007). Simulating the identical physical model with both independent solvers produces similar results (S4), suggesting additional reliability. It also enables us to estimate the uncertainties due to different numerical solvers, never done before in Ganymede's case. A detailed description of our model (S1), a discussion of the uncertainty of upstream conditions and model parameters (S2) and the numerical implementation (S3) is attached in the Supplementary Information. We use the GPhiO coordinates, where the primary direction z is parallel to Jupiter's rotation axis, the secondary direction y is pointing towards Jupiter and x completes the right-handed system in direction of plasma flow.

3 Results

For the time of closest approach (CA) the Jovian background magnetic field was inclined by $\sim20°$ to Ganymede's spin and by $\sim15°$ to Ganymede's dipole axis, leading to a sub-alfvénic interaction that is roughly symmetric to the $y = 0$ plane. Ganymede's magnetosphere is characterized by northern and southern Alfvén wings, both bent in the orbital direction. In Figure 1 they can be identified by a tilted magnetic field and lowered plasma velocity and pressure. The modeled angle (xz-plane projection) between the northern wing and the z axis of $\sim46°$ matches the theoretical value of $46.5°$ based on the theory of Neubauer (1980). Inside the Alfvén wings the plasma velocity is reduced below 50 km/s. The convection through the wings over the poles is slowed and takes about 10 minutes for a distance of 10 R_G. The interaction expands the volume characterized by closed field lines on the upstream side in z direction while it is strongly compressed on the downstream side. This area has a thermal pressure below 1 nPa in Figure 1b. The diameter of Ganymede's magnetosphere is about 4 R_G in the equatorial plane as indicated by the reduced and reversed velocity in Figure 1d. On the downstream side the reduced velocity also indicates a stretched magnetospheric tail with more than 10 R_G length that was crossed by Juno at the location of the red cross.

3.1 Magnetic Topology

In Figure 2 and Movie S1, we display the modeled magnetic field topology together with Juno's trajectory (red) in 3D. The volume of open field lines is represented by the blue surface and was crossed by Juno. In our model the crossings occurred inbound at 16:48:16 on the tail side and at 17:00:16 outbound at the northern Jupiter-facing side. We do not see Juno on closed field lines at any time. The height of the closed field line region, green in Figure 2, increases in upstream direction. Juno's trajectory is located
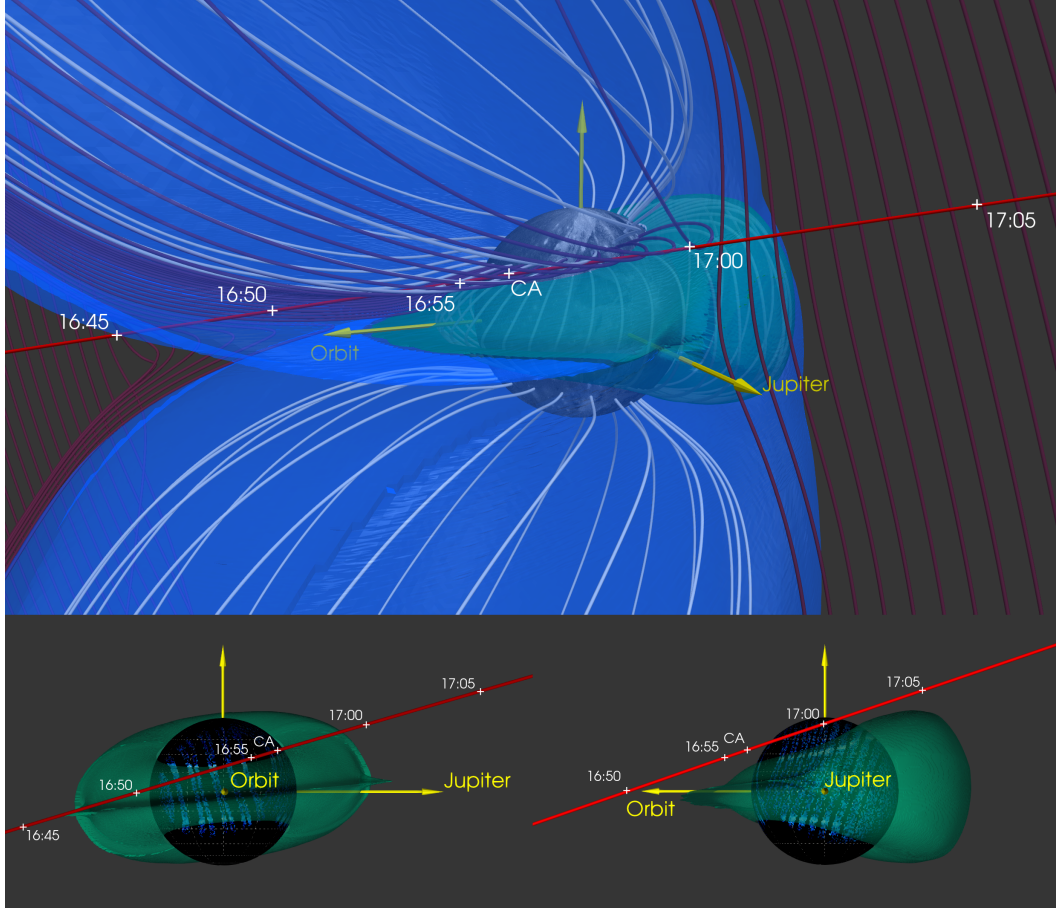
Figure 2. Juno's trajectory (red) in relation to the modeled magnetosphere during the flyby of Ganymede. The timestamps in UTC indicate the position of Juno. In the upper panel the lines show selected magnetic field lines connected to Ganymede's surface (white) and Juno's trajectory (dark). The green surface represents the outer boundary of closed field lines, the blue surface represents the outer boundary of open field lines that connect to Ganymede at one end. The bottom panel additionally shows observed 130.4 and 135.6 nm oxygen emissions from the aurora in blue (Greathouse et al., 2022).

slightly above this boundary and inclined by a similar angle. Therefore the closest distance between Juno and closed field lines was relatively constant below 0.4 R_G for about 7 minutes, with a minimum of $\sim$0.26 R_G at the time of CA (Figure 3).

The two solid green lines in Figure 4 show the location of the OCFB on Ganymede's surface, calculated by field line tracing. The plasma flow generates magnetic stresses which push the OCFB pole-wards on the upstream side and press them together on the downstream side. Here the averaged latitude (between 45° and 135° W longitude) is at 21.2° (north) and -24.4° (south), respectively. Greathouse et al. (2022) compare the OCFB location with Ganymede's aurora observed by Juno, summarized in Section 5. Figure 4 also shows results from alternative simulations with the background field measured approximately 30 minutes before (dotted) and after (dashed) the flyby. As consequence of the field rotation the OCFB lines appear to migrate in opposite directions, west for the northern and east for the southern hemisphere. This is also identifiable by the longitudinal migration of the latitudinal minimums and maximums (before|CA|after): 108°|111°|113° and -88°|-70°|-67° (north), 62°|60°|53° and -107°|-117°|-121° (south).

The lower multicolored line in Figure 4 shows Juno's radially projected trajectory inside the magnetosphere, its endpoints refer to the magnetopause crossings. The crossings also correspond to the blue vertical lines in Figure 3 and the punctures of the blue surface in Figure 2. Tracing the field lines from Juno's position to the surface yields its magnetic footprint, as shown as upper multicolored line in Figure 4. Since the colors indicate the lengths of the field lines between Juno and the surface, the footprint location associated to a fixed position of the spacecraft can be identified by a shared color. Juno's footprint is modeled to be up to 11° and on average 7° degree north of the OCFB as modeled with the estimated background field during CA. During approach to CA Juno's mapped position on the surface was nearly on the same meridian as Juno itself. After CA the field lines become more bent in longitudinal direction (Figure 2) resulting in an eastern shift of Juno's footprint. Juno's footprint touches the OCFB at both ends. While this is counter intuitive at first glance, it is a direct consequence of the magnetic topology. Every magnetopause crossing, although possibly far away from closed field lines, touches an open field line that ends at the OCFB at Ganymede's surface. This convergence of field lines brings the footprints on the surface closer to the OCFB than Juno's position itself.

3.2 Comparison with Magnetometer Measurements

In Figure 3 we compare our modeled magnetic field with Juno's magnetometer (MAG) measurements (J. E. P. Connerney et al., 2017). The blue vertical lines represent the modeled times when Juno entered and left the open field line region, namely the inbound and outbound magnetopause crossings. Although short-term fluctuations are not covered by our model, the overall structure is reproduced very well. The field rotations have a consistent shape and even the rotation in the wake region (16:45) is predicted at the correct time. The latter demonstrates that the increased diameter of the tail structure (Figure 1d) is consistent with the observations. This feature is sensitive to the spatial resolution (see Figure S1). During the actual inbound magnetopause crossing, both the measurements and our model do not indicate a rotation.

We identify two noticeable deviations. (1) The model features a clear outbound crossing but it is located slightly too far inwards and occurs $\sim$40 s too early. We analyze the impact of uncertain upstream conditions on this in Section 4. (2) In the closer vicinity of Ganymede B_z is slightly overestimated by 10 to 20 nT. We found that this deviation is sensitive to the numerical resolution in latitudinal direction, which affects the compression of the closed field line region on the downstream side. We interpret this that a high resolution is required to resolve the strong magnetic stresses at lower latitudes. Our latitudinal resolution is $\sim$0.75°. We expect the B_z deviation might reduce further if an even higher resolution would be feasible.
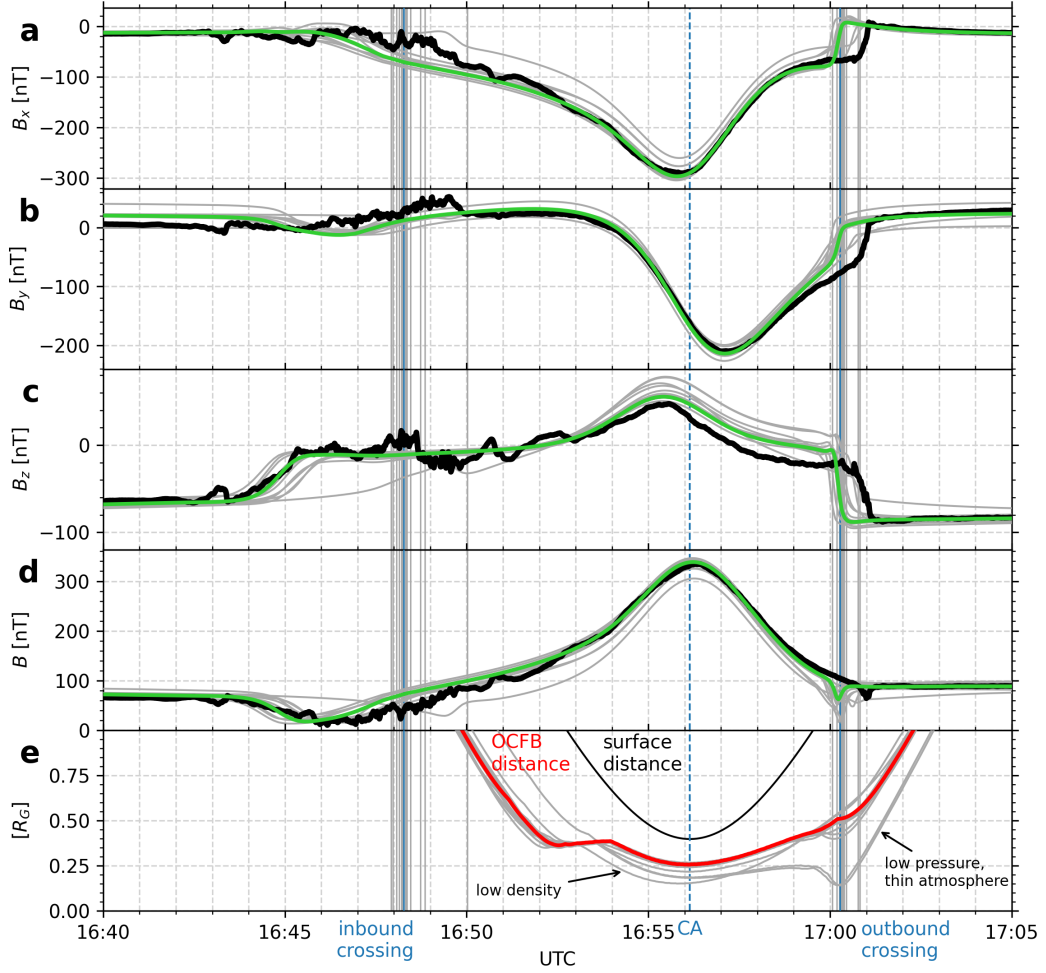
Figure 3. Modeled (green) versus measured (black) magnetic field along Juno's trajectory (panels a-d, GPhiO). Panel e shows Juno's distance from Ganymede's surface (black) and the OCFB (red) in R_G. The blue vertical lines represent the modeled inbound and outbound magnetopause crossings. The gray lines indicate model uncertainty from uncertain upstream conditions (Section 4).
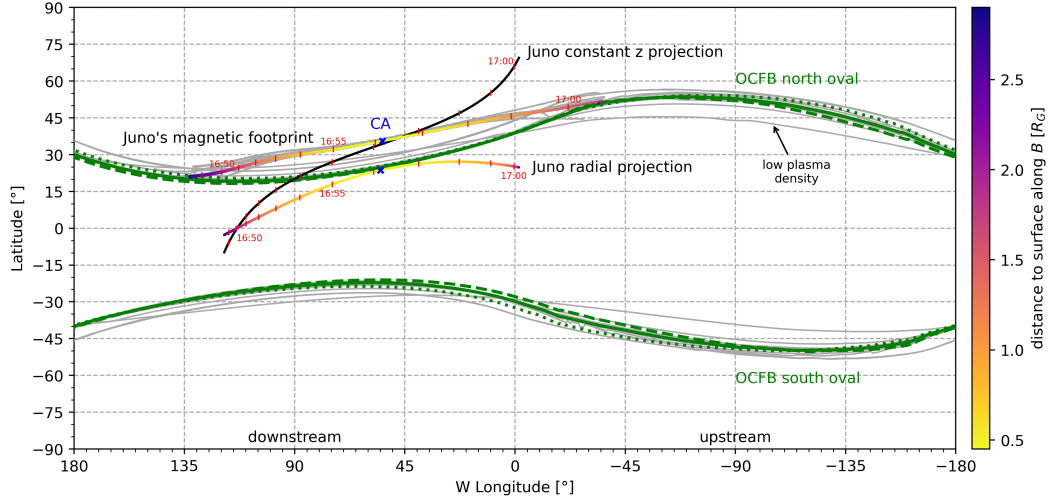
Figure 4. Surface map of Ganymede with 0° longitude pointing towards Jupiter ($+y$ GPhiO). The modeled OCFB from our default model is shown as solid green lines. The dotted (dashed) lines show its location based on modelling with the measured background field before (after) the flyby. Greathouse et al. (2022) show the coincidence of the OCFB and the observed aurora. Juno's position, while inside the magnetosphere, is projected in radial direction and shown as the lower multicolored line, the same with constant z as black line. The upper multicolored line shows the location where field lines end that are connected to Juno, namely Juno's magnetic footprint. Color coded is the distance along those field lines. The gray lines indicate model uncertainty from uncertain upstream conditions (Section 4).

4 Model Sensitivity

For the interpretation of Juno's measurements a model can play an important role. In contrast to measurements, however, it is complex to apply a quantitative error analysis to assess the uncertainty of our quantitative results. Model errors originate from (1) model assumptions, (2) uncertain parameters (this section) and (3) the numerics (Supplementary Information S4).

To investigate error source (2) we carry out a parameter study by varying single parameters to their individual realistic minimum and maximum values as listed in Table 1. This also helps to estimate the model sensitivity on each parameter. The upstream conditions during Juno's flyby are not completely available from direct measurements alone and therefore contain uncertainties of different magnitude, as described in detail in the Supplementary Information (S2). The parameter study also includes uncertainties of the primary dipole moment g_1^0 ($\pm 2\%$) and our parametrizations of the atmospheric density and ionization rate, assuming uncertainties each by a factor of 5.

In the MHD view the locations of magnetopause and OCFB are determined by equilibriums of forces that depend on the physical parameters of the model. Table 1 summarizes the sensitivities of important model results to different parameter variations that are each displayed as gray lines in Figures 3 and 4. A significantly later outbound magnetopause crossing (17:00:49 latest) is modeled if the upstream plasma density is extraordinary low or the measured background field before CA is used. The latter is unlikely to still represent the background field when Juno crossed the magnetopause about 5 minutes after passing CA. With an uncertainty of ∼2 minutes the inbound crossing is more

Table 1. Variations of model parameters and upstream conditions and their effect on presented model results. Columns 3-6 specify the averaged latitude of the northern and southern open closed field line boundary (OCFB) on Ganymede's surface on the upstream (-45° to -135°W) and downstream (45° to 135°W) side. Column 7 lists Juno's closest distance to closed field lines (CF) and columns 8-9 the UTC times of its inbound and outbound magnetopause crossings, respectively. Column 10 lists the RMS between measured and modeled magnetic field between 16:50 and 16:59.

parameter	value	OCFB down N [°]	S [°]	OCFB up N [°]	S [°]	CF [R_G]	magnetopause crossing inbound	outbound	RMS [nT]
default	- [a]	21.2	-24.4	51.5	-47.4	0.26	16:48:16	17:00:16	9.3
B_0 before CA	(-16,3,-70) nT [b]	22.1	-25.4	52.7	-48.4	0.25	16:48:43	17:00:46	12.8
B_0 after CA	(-14,43,-80) nT [b]	20.6	-23.7	50.6	-46.7	0.26	16:48:13	17:00:03	12.0
velocity	120 km/s [c]	22.1	-25.3	50.6	-46.4	0.24	16:48:27	17:00:22	9.7
velocity	160 km/s [c]	20.8	-23.9	52.7	-48.8	0.26	16:48:04	17:00:19	11.0
density	10 amu/cm^3 [d]	26.5	-30.3	43.2	-38.8	0.15	16:50:01	17:00:49	27.4
density	160 amu/cm^3 [c]	20.6	-23.6	53.3	-49.5	0.27	16:47:55	17:00:17	12.6
pressure	1 nPa	25.3	-28.4	54.5	-50.4	0.14	16:48:12	17:00:26	19.5
pressure	5 nPa	21.4	-24.6	50.9	-46.9	0.25	16:48:51	17:00:11	9.7
production	0.5e-8 /s	21.3	-24.5	51.7	-47.6	0.25	16:48:21	17:00:16	9.5
production	10e-8 /s	21.7	-24.9	51.4	-47.3	0.24	16:48:08	17:00:18	9.8
atmosphere	1.6e6 /cm^3	25.4	-28.5	54.7	-50.6	0.14	16:48:19	17:00:23	19.4
atmosphere	40e6 /cm^3	23.4	-26.7	48.6	-44.6	0.22	16:47:58	17:00:20	13.1
dynamo g_1^0	-2%	21.1	-24.3	51.9	-47.8	0.26	16:48:16	17:00:16	9.3
dynamo g_1^0	+2%	21.7	-24.8	51.9	-47.9	0.25	16:48:14	17:00:19	10.4

[a]: default values: (-15,24,-75) nT [b], 140 km/s [c], 100 amu/cm^3, 2.8 nPa [c], 2.2e8 /s, 8e6 /cm^3
[b]: Weber et al. (2022)
[c]: Kivelson et al. (2022)
[d]: Bagenal and Delamere (2011)

sensitive than the outbound crossing (~45 seconds), as expected from the more dynamic tail where Juno entered Ganymede's magnetosphere.

Our model does not see Juno on closed field lines for any of the considered parameter variations. As Figure 3e suggests, the sensitivity of the distance to closed field lines can be divided into two parts. Before ~16:59 the uncertainty is quite constant <0.15 R_G. After ~16:59, around the outbound crossing, when Juno was above the flank of the closed field line region, the uncertainty is larger and especially low plasma pressure and a thinner atmosphere significantly reduce the distance to closed field lines (0.14 R_G). Additionally, but near CA, the distance is also clearly reduced if lower plasma density is used (0.15 R_G). However, the impact of reduced density and plasma pressure on the physics is different. A lower upstream plasma pressure directly affects the equilibrium of forces at the magnetopause. For unchanged magnetic pressure a reduced plasma pressure thus globally shifts the magnetopause and inflates the total magnetosphere. This results not only in earlier inbound and later outbound crossings but also increases the closed field line region, evolving a secondary minimal distance to Juno's trajectory near Juno's outbound crossing and globally shifting the surface OCFB polewards by 3-4° (Table 1). In contrast, a lower upstream density reduces the momentum of the plasma and thus reduces the interaction strength (Saur et al., 2013). As consequence the interaction induced upstream/downstream asymmetry of the closed field line region is weaker. The surface OCFB is shifted 5-6° polewards / 8-9° equatorwards on the downstream / upstream side and Juno's trajectory is closer to closed field lines near CA. Varying the upstream velocity shows similar impact, even if less pronounced due to its weaker uncertainty.

In Figure 4, the gray lines show the OCFB location on Ganymede's surface from all simulations with parameter variations. On the upstream side the OCFB location is most sensitive to a reduced density. The total uncertainty from all parameter variations is ~12° upstream and ~7° for the remaining longitudes. However, the plasma density and velocity have a stronger impact upstream, while the production rate mainly affects the downstream side.

Table 1 also lists the deviation of the modeled ($\mathbf{B}$) from the measured ($\hat{\mathbf{B}}$) magnetic fields, defined by $RMS = \sqrt{\frac{1}{3N} \sum_i^N \|\mathbf{B}_i - \hat{\mathbf{B}}_i\|^2}$. We emphasize that this alone is not an appropriate method to assess a model's capability to reproduce measurements; e.g. models that reproduce measured field rotations slightly shifted in time might have a higher RMS than models without any rotations at all. Therefore we consider only the interval 16:50-16:59 to exclude the predicted boundary crossings. According to this evaluation we find that the default parameter setup indeed fits the MAG data best and the variations that reduce the distance to closed field lines have a strongly increased deviation.

5 Discussion and Conclusions

We performed MHD simulations of Ganymede's magnetosphere which put Juno's observations into a three-dimensional context. Our results help to answer questions that arise from analyzing Juno's measurements.

Until now, an examination of the relation between OCFB and auroral ovals suffered from uncertainties of >10° latitude (McGrath et al., 2013). Greathouse et al. (2022) now present that the auroral ovals, observed by Juno, have a sharp poleward decay and that our modeled surface OCFB matches the bright poleward emission edges in very good agreement. On the downstream side, where the aurora mainly was observed, the latitudinal deviations are <1°. Only the Jupiter facing side features little stronger deviations, where the observations are more patchy and our study suggests an increased sensitivity of the OCFB to varied plasma density. A comparison of our model and Juno's observations thus significantly strengthens the conclusion that Ganymede's aurora is brightest exactly at and inside the OCFB.

The various instruments onboard Juno detected the outbound magnetopause crossing more clearly than the inbound, matching expectations of a more dynamic magnetotail without field rotations through the magnetopause. Our model predicts that Juno left Ganymede's magnetosphere at 17:00:16, 14s earlier than JEDI (Clark et al., 2022), 23s earlier than JADE (Allegrini et al., 2022) and about 40s earlier than MAG (Romanelli et al., 2022) and the Waves instrument (Kurth et al., 2022) identified the outbound crossing. Uncertain model parameters could not explain this deviation, leaving an open question for possible further required physics. Dorelli et al. (2015) for example suggested a thickened double magnetopause induced by the Hall effect at the Jupiter facing side. Except this aspect, our model is in excellent agreement with the Juno MAG and UVS observations.

An entry of Juno into the closed field line region is not consistent with our results. This is also supported by geometrical thoughts as follows. The north-south extent of closed field line region on the downstream side is not expected to increase with distance from the surface. Figures 2 and 4 reveal that for the closer parts inside the magnetosphere Juno's trajectory, projected with constant z to the surface, was obviously located north of the aurora and correlated surface OCFB and therefore clearly outside the closed field line region.

We assessed model uncertainties through a sensitivity study to uncertain upstream conditions and model parameters, to our knowledge the first of Ganymede's magneto-

sphere. Our conclusions are robust to these uncertainties and we provide margins for the quantitative results. We found that the variations of all upstream parameters within expected ranges significantly affect different aspects of the magnetosphere and no parameter stands out in its importance. This is also important for the interpretation of the upcoming orbital JUICE or remote-sensing observations without joint in-situ measurements of upstream conditions.

Open Research

The MHD simulation codes utilized for this work are open-source projects. PLUTO can be downloaded at http://plutocode.ph.unito.it/ (version 4.4). ZEUS-MP is available at http://www.netpurgatory.com/zeusmp.html (version 2.1.2). Juno MAG data are publicly available through the Planetary Data System (https://pds-ppi.igpp.ucla.edu/) at https://doi.org/10.17189/1519711 (J. Connerney, 2017). The OCFB and Juno's footprint locations on Ganymede's surface data calculated in this study are available at a Zenodo repository via https://doi.org/10.5281/zenodo.7096938 with CCA 4.0 licence (Duling et al., 2022a). The complete simulation output data of our default model are available at a Zenodo repository via https://doi.org/10.5281/zenodo.7105334 with CCA 4.0 licence (Duling et al., 2022b).

References

Allegrini, F., Bagenal, F., Ebert, R., Louarn, P., McComas, D. J., Szalay, J., . . . Waite, J. H. (2022). Plasma observations during the june 7, 2021 ganymede flyby from the jovianauroral distributions experiment (jade) on juno. *Geophysical Research Letters*, *this issue*.

Bagenal, F., & Delamere, P. A. (2011, may). Flow of mass and energy in the magnetospheres of jupiter and saturn. *Journal of Geophysical Research: Space Physics*, *116*(A5). doi: 10.1029/2010ja016294

Clark, G., Mauk, B. H., Paranicas, C., Kollmann, P., Haggerty, D., Rymer, A., . . . Turner, D. L. (2022). Energetic charged particle observations during juno's close flyby of ganymede. *Geophysical Research Letters*, *this issue*.

Connerney, J. (2017). *Juno mag calibrated data j v1.0, jno-j-3-fgm-cal-v1.0.* NASA Planetary Data System. doi: 10.17189/1519711

Connerney, J. E. P., Benn, M., Bjarno, J. B., Denver, T., Espley, J., Jorgensen, J. L., . . . Smith, E. J. (2017, feb). The juno magnetic field investigation. *Space Science Reviews*, *213*(1-4), 39–138. doi: 10.1007/s11214-017-0334-z

Dorelli, J. C., Glocer, A., Collinson, G., & Tóth, G. (2015, jul). The role of the hall effect in the global structure and dynamics of planetary magnetospheres: Ganymede as a case study. *Journal of Geophysical Research: Space Physics*, *120*(7), 5377–5392. doi: 10.1002/2014ja020951

Duling, S., Saur, J., Clark, G., Allegrini, F., Greathouse, T., Gladstone, R., . . . Sulaiman, A. H. (2022a). *Mhd model of ganymede's magnetosphere: Predicted ocfb and magnetic footprint surface locations for juno's flyby.* Zenodo. Retrieved from `https://doi.org/10.5281/zenodo.7096938` doi: 10.5281/zenodo.7096938

Duling, S., Saur, J., Clark, G., Allegrini, F., Greathouse, T., Gladstone, R., . . . Su-

laiman, A. H. (2022b). *Mhd model output for ganymede's magnetosphere during juno's flyby.* Zenodo. Retrieved from `https://doi.org/10.5281/zenodo.7105334` doi: 10.5281/zenodo.7105334

Duling, S., Saur, J., & Wicht, J. (2014, jun). Consistent boundary conditions at nonconducting surfaces of planetary bodies: Applications in a new ganymede MHD model. *Journal of Geophysical Research: Space Physics*, *119*(6), 4412–4440. doi: 10.1002/2013ja019554

Ebert, R. W., Fuselier, S., Allegrini, F., Angold, N., Bagenal, F., Bolton, S. J., . . . Wilson, R. J. (2022). Evidence for magnetic reconnection at ganymede's upstream magnetopause during the pj34 juno flyby. *Geophysical Research Letters*, *this issue*.

Fatemi, S., Poppe, A. R., Khurana, K. K., Holmström, M., & Delory, G. T. (2016, may). On the formation of ganymede's surface brightness asymmetries: Kinetic simulations of ganymede's magnetosphere. *Geophysical Research Letters*, *43*(10), 4745–4754. doi: 10.1002/2016gl068363

Feldman, P. D., McGrath, M. A., Strobel, D. F., Moos, H. W., Retherford, K. D., & Wolven, B. C. (2000, jun). HST/STIS ultraviolet imaging of polar aurora on ganymede. *The Astrophysical Journal*, *535*(2), 1085–1090. doi: 10.1086/308889

Frank, L. A., Paterson, W. R., Ackerson, K. L., & Bolton, S. J. (1997, sep). Low-energy electron measurements at ganymede with the galileo spacecraft: Probes of the magnetic topology. *Geophysical Research Letters*, *24*(17), 2159–2162. doi: 10.1029/97gl01632

Greathouse, T. K., Gladstone, R., Molyneux, P. M., Versteeg, M. H., Hue, V., Kammer, J., . . . Duling, S. (2022). Uvs observations of ganymede's aurora during juno orbits 34 and 35. *Geophysical Research Letters*, *this issue*.

Gurnett, D. A., Kurth, W. S., Roux, A., Bolton, S. J., & Kennel, C. F. (1996, dec). Evidence for a magnetosphere at ganymede from plasma-wave observations by the galileo spacecraft. *Nature*, *384*(6609), 535–537. doi: 10.1038/384535a0

Hall, D. T., Feldman, P. D., McGrath, M. A., & Strobel, D. F. (1998, may). The far-ultraviolet oxygen airglow of europa and ganymede. *The Astrophysical Journal*, *499*(1), 475–481. doi: 10.1086/305604

Hansen, C. J., Bolton, S., Sulaiman, A., Duling, S., Brennan, M., Connerney, J., . . . Withers, P. (2022). Juno's close encounter with ganymede - an overview. *Geophysical Research Letters*, *this issue*.

Hayes, J. C., Norman, M. L., Fiedler, R. A., Bordner, J. O., Li, P. S., Clark, S. E., . . . Low, M.-M. M. (2006, jul). Simulating radiating and magnetized flows in multiple dimensions with ZEUS-MP. *The Astrophysical Journal Supplement Series*, *165*(1), 188–228. doi: 10.1086/504594

Jia, X., Walker, R. J., Kivelson, M. G., Khurana, K. K., & Linker, J. A. (2008, jun). Three-dimensional MHD simulations of ganymede's magnetosphere. *Journal of Geophysical Research: Space Physics*, *113*(A6), n/a–n/a. doi: 10.1029/2007ja012748

Jia, X., Walker, R. J., Kivelson, M. G., Khurana, K. K., & Linker, J. A. (2009, sep). Properties of ganymede's magnetosphere inferred from improved three-dimensional MHD simulations. *Journal of Geophysical Research: Space Physics*, *114*(A9), n/a–n/a. doi: 10.1029/2009ja014375

Kivelson, M. G., Bagenal, F., Jia, X., Khurana, K., Volwerk, M., & Zarka, P. (2022). Ganymede's magnetosphere and its interaction with the jovian magnetosphere. In M. Volwerk & M. McGrath (Eds.), *Ganymede.* Cambridge, UK: Cambridge University Press.

Kivelson, M. G., Bagenal, F., Kurth, W. S., Neubauer, F. M., Paranicas, C., & Saur, J. (2004). Magnetispheric interaction with satellites. In *Jupiter - the planet, satellites and magnetosphere* (p. 513-536). Cambridge Univ. Press, New York.

Kivelson, M. G., Khurana, K., & Volwerk, M. (2002, jun). The permanent and in-

ductive magnetic moments of ganymede. *Icarus*, *157*(2), 507–522. doi: 10 .1006/icar.2002.6834

Kivelson, M. G., Khurana, K. K., Coroniti, F. V., Joy, S., Russell, C. T., Walker, R. J., . . . Polanskey, C. (1997, sep). The magnetic field and magneto- sphere of ganymede. *Geophysical Research Letters*, *24*(17), 2155–2158. doi: 10.1029/97gl02201

Kivelson, M. G., Khurana, K. K., Russell, C. T., Walker, R. J., Warnecke, J., Coroniti, F. V., . . . Schubert, G. (1996, dec). Discovery of ganymede's magnetic field by the galileo spacecraft. *Nature*, *384*(6609), 537–541. doi: 10.1038/384537a0

Kurth, W., Sulaiman, A., Hospodarsky, G. B., Menietti, J., Mauk, B. H., Clark, G., . . . Louis, C. (2022). Juno plasma wave observations at ganymede. *Geophysical Research Letters*, *this issue*.

Marconi, M. (2007, sep). A kinetic model of ganymede's atmosphere. *Icarus*, *190*(1), 155–174. doi: 10.1016/j.icarus.2007.02.016

Mauk, B. H. (2004). Energetic ion characteristics and neutral gas interactions in jupiter's magnetosphere. *Journal of Geophysical Research*, *109*(A9). doi: 10 .1029/2003ja010270

McGrath, M. A., Jia, X., Retherford, K., Feldman, P. D., Strobel, D. F., & Saur, J. (2013, may). Aurora on ganymede. *Journal of Geophysical Research: Space Physics*, *118*(5), 2043–2054. doi: 10.1002/jgra.50122

Mignone, A., Bodo, G., Massaglia, S., Matsakos, T., Tesileanu, O., Zanni, C., & Ferrari, A. (2007, may). PLUTO: A numerical code for computational astro- physics. *The Astrophysical Journal Supplement Series*, *170*(1), 228–242. doi: 10.1086/513316

Neubauer, F. (1980, mar). Nonlinear standing alfvén wave current system at io: Theory. *Journal of Geophysical Research: Space Physics*, *85*(A3), 1171–1178. doi: 10.1029/ja085ia03p01171

Paty, C. (2004). Multi-fluid simulations of ganymede's magnetosphere. *Geophysical Research Letters*, *31*(24). doi: 10.1029/2004gl021220

Romanelli, N., DiBraccio, G. A., Modolo, R., Connerney, J. E. P., W.Ebert, R., Martos, Y. M., . . . Bolton, S. J. (2022). Analysis of juno magnetometer observations:comparisons with a global hybrid simulation andindications of ganymede's magnetopause reconnection. *Geophysical Research Letters*, *this issue*.

Roth, L., Ivchenko, N., Gladstone, G. R., Saur, J., Grodent, D., Bonfond, B., . . . Retherford, K. D. (2021, jul). A sublimated water atmosphere on ganymede detected from hubble space telescope observations. *Nature Astronomy*, *5*(10), 1043–1051. doi: 10.1038/s41550-021-01426-9

Saur, J., Duling, S., Roth, L., Jia, X., Strobel, D. F., Feldman, P. D., . . . Hartkorn, O. (2015, mar). The search for a subsurface ocean in ganymede with hub- ble space telescope observations of its auroral ovals. *Journal of Geophysical Research: Space Physics*, *120*(3), 1715–1737. doi: 10.1002/2014ja020778

Saur, J., Grambusch, T., Duling, S., Neubauer, F. M., & Simon, S. (2013, apr). Magnetic energy fluxes in sub-alfvénic planet star and moon planet inter- actions. *Astronomy & Astrophysics*, *552*, A119. doi: 10.1051/0004-6361/ 201118179

Tóth, G., Jia, X., Markidis, S., Peng, I. B., Chen, Y., Daldorff, L. K. S., . . . Dorelli, J. C. (2016, feb). Extended magnetohydrodynamics with embedded particle-in- cell simulation of ganymede's magnetosphere. *Journal of Geophysical Research: Space Physics*, *121*(2), 1273–1293. doi: 10.1002/2015ja021997

Wang, L., Germaschewski, K., Hakim, A., Dong, C., Raeder, J., & Bhattacharjee, A. (2018, apr). Electron physics in 3-d two-fluid 10-moment modeling of ganymede's magnetosphere. *Journal of Geophysical Research: Space Physics*, *123*(4), 2815–2830. doi: 10.1002/2017ja024761

440   Weber, T., Moore, K., Connerney, J., Espley, J., DiBraccio, G., & Romanelli, N.
441   (2022). Updated spherical harmonic moments of ganymedefrom the juno flyby.
442   *Geophysical Research Letters*, *this issue*.
443   Williams, D. J., Mauk, B. H., McEntire, R. W., Roelof, E. C., Armstrong, T. P.,
444   Wilken, B., . . . Murphy, N. (1997, sep). Energetic particle signatures at
445   ganymede: Implications for ganymede's magnetic field. *Geophysical Research*
446   *Letters*, *24*(17), 2163–2166. doi: 10.1029/97gl01931